Journal of Alloys and Compounds 509 (2011) 5893–5896

Contents lists available at ScienceDirect

Journal of Alloys and Compounds

journal homepage: www.elsevier.com/locate/jallcom

Magnetic properties of Sn–Mg substituted strontium hexaferrite nanoparticles synthesized via coprecipitation method

A. Davoodi, B. Hashemi*

Department of Materials Science and Engineering, School of Engineering, Shiraz University, Shiraz, Iran

ARTICLE INFO

Article history:
Received 30 November 2010
Received in revised form 5 January 2011
Accepted 1 March 2011

Keywords:
Permanent magnets
Chemical synthesis
Anisotropy
Magnetic measurements

ABSTRACT

Nanoparticles of Sn–Mg substituted strontium hexaferrite with the composition of $SrFe_{12-x}(Sn_{0.5}Mg_{0.5})_xO_{19}$ ($x = 0.0$–1.0) were synthesized by chemical coprecipitation method. Deionized water/ethanol (50/50) was used as the solvent. The single phase strontium hexaferrites were obtained at pH 13 and Fe^{3+}/Sr^{2+} molar ratio of 9 after calcination at 800 °C. The mean particle size of samples was decreased from 82 to 56 nm with increasing the Sn–Mg content from $x = 0.0$ to $x = 0.8$. The effect of Sn–Mg substitution on magnetic properties of hexaferrites was studied using vibrating-sample magnetometer. It was found that increasing the Sn–Mg from $x = 0.0$ to $x = 0.8$ reduced the coercivity from 4728.9 to 1455.5 Oe and increased the saturation magnetization from 51.34 to 65.49 emu/g. A vector network analyzer was used to investigate the microwave absorption properties. According to microwave measurements, doped strontium hexaferrite composites had much more effective electromagnetic absorption properties than undoped strontium hexaferrite composite.

1. Introduction

The M-type ferrites with magnetoplumbite structure and composition of $MFe_{12}O_{19}$ (M = Sr, Ba, Pb) have been studied because of high Curie temperature, relatively large magnetization, excellent chemical stability and high microwave magnetic loss [1,2]. Strontium hexaferrite nanoparticles have a wide range of uses in several applications such as magnetic recording media, microwave devices and microelectromechanical systems (MEMS) [3,4]. The orientation of spins and location of magnetic ions in the crystal lattice have been determined by Gorter [3]. The unit cell of this structure consists of ten oxygen layers. Within these layers, the Fe^{3+} ions occupy five different interstitial sites. Three sites, named 2a, 12k, and $4f_2$ have octahedral coordination, one site ($4f_1$) has tetrahedral coordination and the 2b site has trigonal bipyramidal (Fivefold) coordination. The Fe^{3+} ions in the 2a, 12k and 2b sites are aligned parallel to each other whereas those of $4f_1$ and $4f_2$ are arranged in opposite directions. The magnetic properties of M-type ferrites depend on synthesis procedure, particle size, composition and substitution of Fe^{3+} ions with other cations at five interstitial sites. A conventional route for the synthesis of strontium hexaferrite involves a solid-state reaction of iron oxide and strontium carbonate mixture at around 1200 °C [5]. However, preparation of chemically homogeneous, strain free and mono-dispersed nanoparticles could not be easy via conventional methods. Consequently, several methods to synthesize these materials have been investigated [6–10]. Among them, coprecipitation as a simple and low cost method has been recently attracted much attention [11,12]. For improvement of magnetic properties of strontium hexaferrites the substitution of several cations such as Al^{3+}–Ga^{3+}, Zr^{4+}–Zn^{2+}, Zr^{4+}–Ni^{2+} at five interstitial sites of hexaferrite have been investigated [13–16]. In the case of M-type hexaferrites, it was known that the crystalline anisotropy could be reduced by Sn^{4+}–Zn^{2+}, Sn^{4+}–Co^{2+}, Sn^{4+}–Mn^{2+} and Sn^{4+}–Ni^{2+} substitution of Fe^{3+} ions [17–19]. Reduction in anisotropy decreases the coercivity but replacement of Fe^{3+} by these cations lowers the saturation magnetization. Low coercivity and high saturation magnetization values are simultaneously required for use in recording media applications [14]. Accordingly, reduction in the coercivity along with increasing in the saturation magnetization is a new approach in preparing hexaferrites. The aim of the present study was to investigate the influence of Sn–Mg substitution on the structure, particle size and magnetic properties of coprecipitated strontium hexaferrite nanoparticles.

2. Experimental

High purity materials, $Fe(NO_3)_3.9H_2O$ (Merck, >99%), $Sr(NO_3)_2$ (Merck, >99%), $SnCl_4$ (Merck, >99%), $Mg(C_2H_3O_2)_2.4H_2O$ (Merck, >99.5%) and NaOH (Merck, >99%) were used in the synthesis of samples. Initially iron nitrate and strontium nitrate with Fe^{3+}/Sr^{2+} molar ratio of 9 were dissolved in a mixture of deionized water/ethanol (50/50) as the solvent. Then tin chloride and magnesium acetate were added to the solvent to achieve stoichiometry of $SrFe_{12-x}(Sn_{0.5}Mg_{0.5})_xO_{19}$ where $x = 0.0$–1.0. The hexaferrite precursors were precipitated by addition of NaOH solution (2 M) as a precipitating agent at pH 13. After drying at 80 °C, the precipitates

* Corresponding author. Tel.: +98 7116133399; fax: +98 7112307293.
E-mail address: hashemib@shirazu.ac.ir (B. Hashemi).

0925-8388/$ – see front matter © 2011 Elsevier B.V. All rights reserved.
doi:10.1016/j.jallcom.2011.03.002

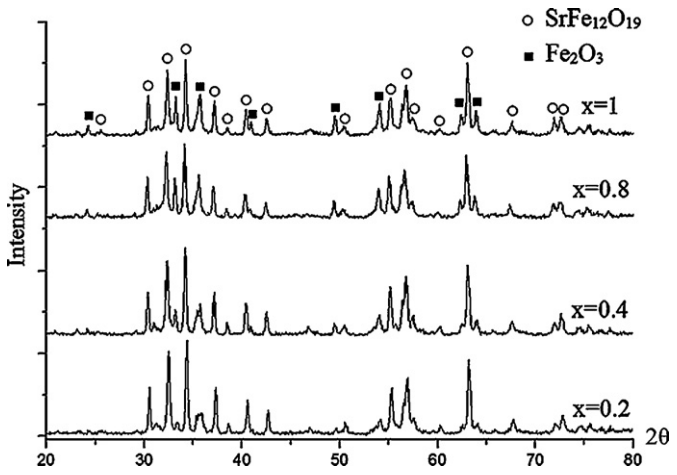

Fig. 1. The X-ray diffraction patterns of the samples with different Sn–Mg substitution levels after calcination at 700 °C for 2 h.

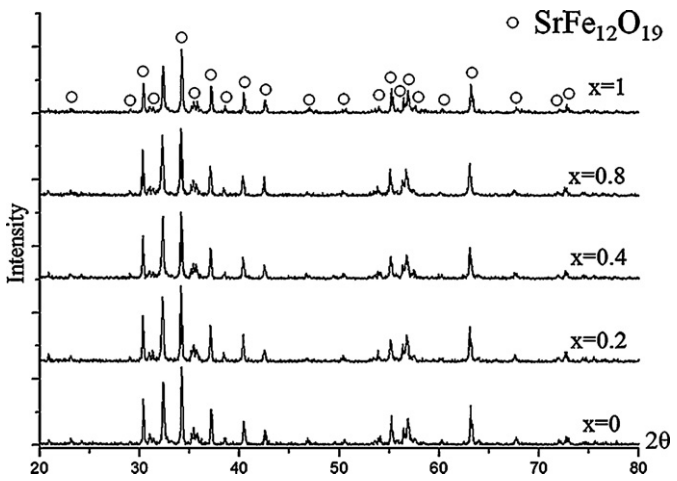

Fig. 2. The X-ray diffraction patterns of the strontium hexaferrites with different Sn–Mg substitution levels, after calcination at 800 °C for 2 h.

were calcined at 700 and 800 °C for 2 h. In order to measure the microwave absorbing properties of hexaferrite, the composite specimens were prepared by mixing strontium hexaferrite powders and an acrylic resin with the weight ratio of 70:30 respectively. Mixtures of ferrite powders with acrylic resin were plasticized and fired at 240 °C and 6 Mpa. The formed composites were cylindrical with the thickness of 2 mm and the diameter of 10 mm. The phase composition of samples was determined by X-ray diffraction (XRD). A Bruker, D8 advanced X-ray diffractometer (with Cu Kα radiation) was used. The elemental composition was determined with X-ray fluorescence analysis (XRF, Bruker S4 Explorer). A Leica Cambridge S-360 scanning electron microscope (SEM) and a dynamic light scattering nanoparticles size analyzer (Horiba LB-550) were used to measure the particle size of the samples. The magnetic properties were measured using a vibrating sample magnetometer (VSM) with maximum field strength of 1 T (10,000 Oe). A vector network analyzer was used to investigate the microwave absorption properties of the composite specimens.

3. Results and discussion

The X-ray diffraction patterns of the samples with different Sn–Mg substitution levels calcined at 700 °C are shown in Fig. 1. It is evident that all of the samples are mixtures of $SrFe_{12}O_{19}$ and Fe_2O_3 phases, and the proportion of Fe_2O_3 phase increased with increasing the substitution level from $x = 0.2$ to $x = 1.0$.

Fig. 2 shows the X-ray diffraction patterns of the substituted strontium hexaferrite samples after calcination at 800 °C for 2 h. As seen, X-ray patterns of all samples are corresponding to the $SrFe_{12}O_{19}$ phase [20] and other phases are not seen. Accordingly, the single phase Sn–Mg substituted strontium hexaferrite samples

Table 1
The elemental composition of $SrFe_{12-x}(Sn_{0.5}\ Mg_{0.5})_xO_{19}$ ($x = 0.0$, 0.2 and 1.0) samples determined by XRF analysis and nominal composition of them.

$X = 1.0$		$X = 0.2$		$X = 0.0$		
Nomminal composition	XRF analysis	Nomminal composition	XRF analysis	Nomminal composition	XRF analysis	Element
11	10.83	11.8	11.65	12	11.86	Fe
1	1.08	1	1.11	1	1.07	Sr
0.5	0.53	0.1	0.11	0	0	Sn
0.5	0.56	0.1	0.13	0	0	Mg

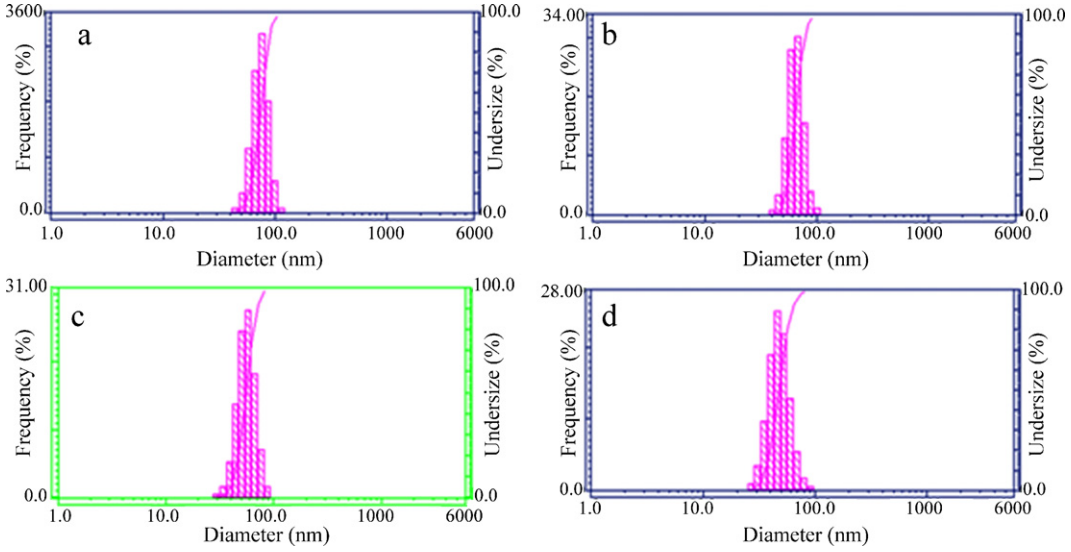

Fig. 3. Size distribution of the substituted strontium hexaferrites $SrFe_{12-x}(Sn_{0.5}\ Mg_{0.5})_xO_{19}$ with $x = 0.0$ (a), $x = 0.4$ (b), $x = 0.6$ (c) and $x = 0.8$ (d).

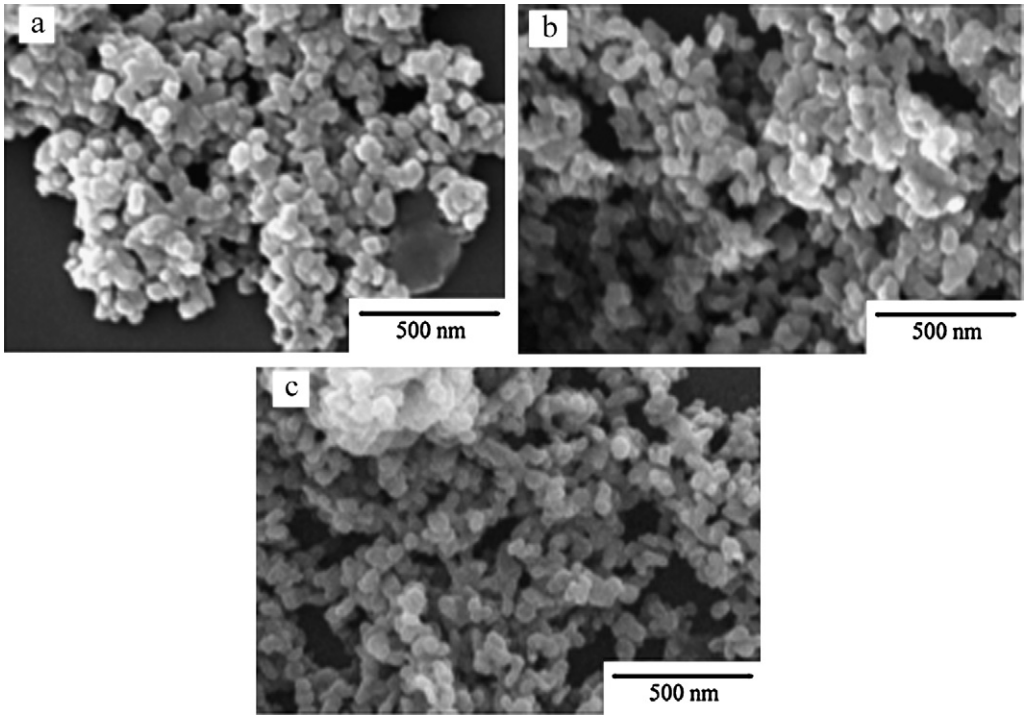

Fig. 4. SEM micrographs of $SrFe_{12-x}(Sn_{0.5}\ Mg_{0.5})_xO_{19}$ samples synthesized with $x = 0.0$ (a), $x = 0.6$ (b) and $x = 0.8$ (c).

were obtained by increasing the calcination temperature from 700 to 800 °C.

The results of XRF elemental composition analysis of $SrFe_{12-x}(Sn_{0.5}\ Mg_{0.5})_xO_{19}$ (where $x = 0.0$, 0.2 and 1.0) samples are presented in Table 1. The elemental composition results are in good agreement with the nominal composition of hexaferrites.

The mean particle size and particle size distribution of Sn–Mg substituted strontium hexaferrite samples are shown in Fig. 3. It was found that the mean particle size of samples decreased by increasing the substitution level. The mean particle sizes of samples with $x = 0.0$, 0.4, 0.6 and 0.8 were 82, 69, 61 and 56 nm, respectively. It may be due to effect of pH of precursors. When tin chloride and magnesium acetate were added to the solvent, pH decreases to lower values and higher amount of NaOH is required to reach pH 13. Therefore it could change the nucleation rate of precipitation during ferrite synthesizes. Narrow particle size distribution of powders can satisfy the requirement for specific applications [21].

Fig. 4 shows the SEM micrographs of the Sn–Mg substituted strontium hexaferrites calcined at 800 °C for 2 h. An image analyzer was used to estimate the mean particle size of the samples. The mean particle sizes of samples with $x = 0.0$, 0.6 and 0.8 were 69, 55 and 48 nm, respectively. The obtained results are in accordance with those of PSA. The small difference between the results could be due to agglomeration of particles in PSA. Again, the measurements showed that the mean particle size of hexaferrite was decreased by increasing the Sn–Mg content and it was in agreement with other researches [22].

The magnetic properties of the Sn–Mg substituted samples were presented in Figs. 5 and 6. Fig. 5 shows the M–H hysteresis curves of the $SrFe_{12-x}(Sn_{0.5}\ Mg_{0.5})_xO_{19}$ powders where $x = 0.0$–0.8. The samples could not be saturated completely due to insufficient magnetic field of 1 Tesla (10,000 Oe). The effects of Sn–Mg substitution on the coercivity and saturation magnetization of samples were summarized in Fig. 6. The obtained results showed that the coercivity was decreased from 4728.9 to 1455.5 Oe by increasing the Sn–Mg proportion from $x = 0$ to $x = 0.8$. It has been shown the coercivity of hexaferrites is dependent on the crystalline and shape anisotropy [19]. As it has been reported [14,15,19] substitution of Fe^{3+} from octahedral sites by nonmagnetic cations causes the crystalline anisotropy decreases and anisotropy changes from uniaxial to planar. Reduction in the coercivity could be a consequent of this replacement. On the other hand, the shape anisotropy can be reduced by decreasing the particle size. Accordingly, decreasing particle size with increasing Sn–Mg content could be another reason for decrease of the coercivity.

It is also obvious that the saturation magnetization increases from 51.34 to 65.49 emu/g with increasing the Sn–Mg values from $x = 0.0$ to $x = 0.8$. This is in good agreement with Ghasemi et al. report [23]. The Sn^{+4} and Mg^{+2} cations usually occupy the octahedral sites. The $4f_2$ has an opposite spin relative to other octahedral sites. Therefore, increase in saturation magnetization may be due to replacement of Fe^{+3} from $4f_2$ sites by nonmagnetic Sn^{+4} and

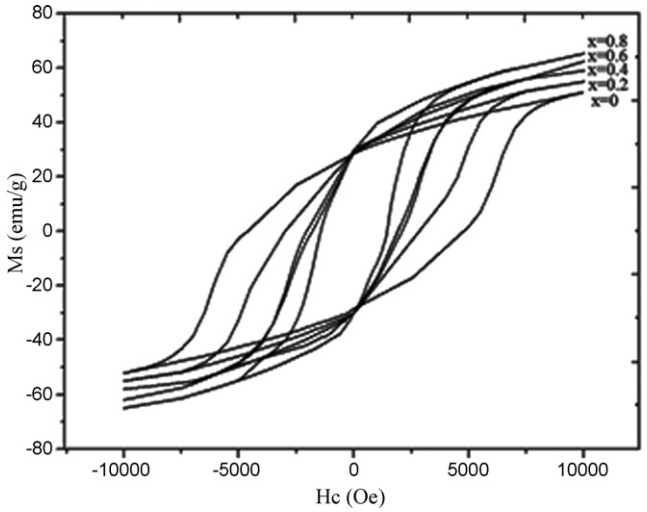

Fig. 5. Hysteresis curves of the strontium hexaferrite samples synthesized with different Sn–Mg substitution levels.

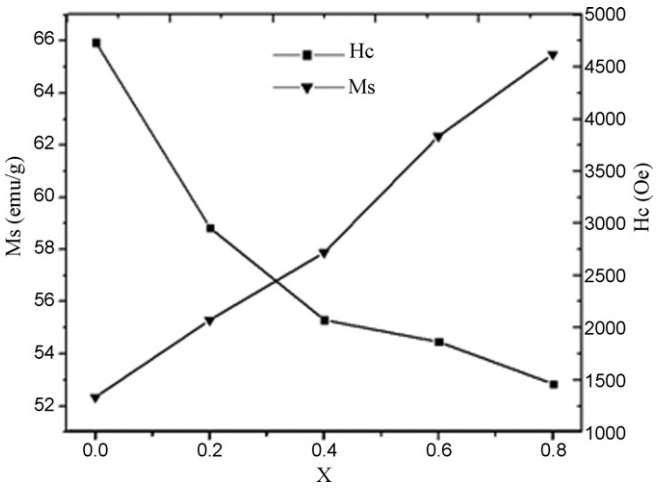

Fig. 6. Effect of Sn–Mg substitution on the coercivity and saturation magnetization of hexaferrites.

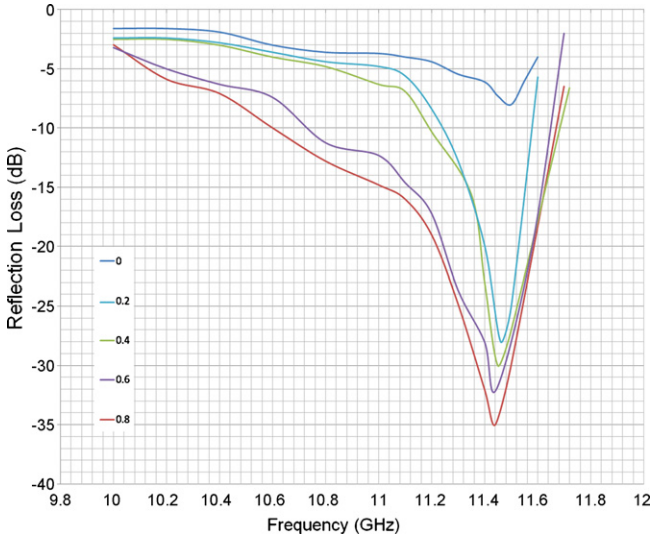

Fig. 7. Reflection loss versus frequency in the composite samples with different Sn^{+4} and Mg^{+2} substituted hexaferrites.

Mg^{+2} cations. This replacement is in accordance with previous argument related to decrease in coercivity.

Fig. 7 shows the variation of reflection loss with the frequency in the composite samples with a proportion of 70 wt% ferrites. For microwave applications, the reflection loss should be more than −20 dB. The bandwidth is the frequency range that the reflection loss is more than −20 dB. The bandwidth and reflection loss of the composite containing undoped hexaferrite is not appropriate for use as microwave absorption materials. This is due to high anisotropy fields of ferrite. The natural resonance and domain wall resonance are two different resonance mechanisms in polycrystalline ferrites. The natural resonance is usually higher than domain wall resonance. The natural resonance frequency, f_r, is dependent on anisotropies as the following equation:

$$2\pi f_r = \gamma(H_\Theta H_\Phi)^{1/2}$$

where γ is the gyromagnetic ratio, H_Θ is out of plane anisotropy field and H_Φ is in plane anisotropy field [23]. Therefore, with Sn^{+4} and Mg^{+2} substitutions, the anisotropy fields decrease and according to performed studies the anisotropy is modified from uniaxial to nearly planar [19,23]. Consequently, the corresponding natural resonance frequencies should be decreased. For the composite containing doped ferrite with $x = 0.2$ the matching frequencies and reflection loss are equal to 11.46 GHz and −28 dB. At relatively same frequencies, the reflection loss reach −29.5 and −32 for $x = 0.4$ and 0.6, respectively. The bandwidth increases with Sn^{+4} and Mg^{+2} content. The composite containing doped ferrite with $x = 0.8$ had the highest reflection loss and bandwidth. The maximum reflection loss was −35 dB at a matching frequency of 11.44 GHz.

4. Conclusion

Single phase nanoparticles of Sn–Mg substituted strontium hexaferrites were synthesized successfully by a coprecipitation method. Good agreement was observed between the XRF analysis and nominal elemental composition of hexaferrites. The influences of Sn–Mg substitution on the particle size and magnetic properties of coprecipitated strontium hexaferrite nanoparticles were studied. The mean particle size of samples was decreased from 82 to 56 nm with increasing the Sn–Mg content from $x = 0.0$ to $x = 0.8$. It was found that increasing the Sn–Mg content from $x = 0.0$ to $x = 0.8$ led to a reduction in the coercivity from 4728.9 to 1455.5 Oe and increasing the saturation magnetization from 51.34 to 65.49 emu/g. Accordingly, the synthesized hexaferrites can satisfy the requirements for applications in recording media. Based on microwave measurements, the composites from doped strontium hexaferrite and acrylic resin could be suitable for practical applications at high frequencies. It was concluded that the composites containing doped ferrites had much more effective electromagnetic absorption properties. The composites which contained doped ferrite with $x = 0.8$ exhibited the largest reflection loss and the widest bandwidth relative to other specimens.

References

[1] N. Dishovske, A. Petkov, I. Nedkov, I. Razkazov, IEEE Trans. Magn. 30 (1994) 969–971.
[2] S.R. Janasi, M. Emura, F.J.G. Landgraf, D. Rodrigues, J. Magn. Magn. Mater. 238 (2002) 168–172.
[3] H. Kojima, in: E.P. Wohlfarth (Ed.), A Handbook on the Properties of Magnetically Ordered Substances, North-Holland, Amsterdam, 1982.
[4] X.X. Liu, J.M. Bai, F.L. Wei, Z. Yang, A. Morisako, M. Matsunori, J. Magn. Magn. Mater. 212 (2000) 273–275.
[5] M. Radwan, M.M. Rashad, M.M. Hessien, J. Mater. Process. Technol. 181 (2007) 106–109.
[6] D. Lisjak, M. Drofenik, J. Eur. Ceram. Soc. 26 (2006) 3681–3686.
[7] A. Ataie, M.R. Piramoon, I.R. Harris, C.B. Ponton, J. Mater. Sci. 30 (1995) 5600–5606.
[8] J. Fang, J. Wang, L. Gan, S. Ng, J. Ding, X. Liu, J. Am. Ceram. Soc. 83 (2000) 1049–1055.
[9] R. Müller, J. Magn. Magn. Mater. 101 (1991) 230–232.
[10] M. Jean, V. Nachbaur, J. Bran, J.M. Breton, J. Alloys Compd. 496 (2010) 306–312.
[11] M.M. Hessien, M.M. Rashad, K. El-Barawy, J. Magn. Magn. Mater. 320 (2008) 336–343.
[12] C.W. Chang, M.S. Tzeng, S.J. Wang, J. Mater. Sci. Lett. 9 (1990) 832–835.
[13] M.J. Iqbal, M.N. Ashiq, J. Magn. Magn. Mater. 320 (2008) 881–886.
[14] M.J. Iqbal, M.N. Ashiq, P.H. Gomez, J. Alloys Compd. 478 (2009) 736–740.
[15] M.J. Iqbal, M.N. Ashiq, P.H. Gomez, J. Scr. Mater. 57 (2007) 1093–1096.
[16] Z. Pang, X. Zhang, B. Ding, J. Alloys Compd. 492 (2010) 691–694.
[17] D.H. Han, Z. Yang, H.X. Zeng, X.Z. Zhou, A.H. Morrish, J. Magn. Magn. Mater. 137 (1994) 191–196.
[18] H.C. Fang, Z. Yang, C.K. Ong, Y. Li, C.S. Wang, J. Magn. Magn. Mater. 187 (1998) 129–135.
[19] D. Lisjak, M. Drofenik, J. Eur. Ceram. Soc. 24 (2004) 1841–1845.
[20] P.B. Braun, Philips Res. Rep. 12 (1957) 491–548.
[21] J.F. Wang, C.B. Ponton, I.R. Harris, J. Magn. Magn. Mater. 242–245 (2002) 1464–1467.
[22] T.S. Chin, M.C. Deng, S.L. Hsu, IEEE Trans. Magn. 29 (1993) 3644–3646.
[23] A. Ghasemi, X. Liu, A. Morisako, IEEE Trans. Magn. 45 (2009) 4420–4423.